Enhanced wear and corrosion resistance of plasma electrolytic carburized layer on T8 carbon steel

Jie Wu [a, b], Bin Wang [a, b], Yifan Zhang [a, b], Run Liu [a, b], Yuan Xia [c], Guang Li [c], Wenbin Xue [a, b, *]

[a] Key Laboratory for Beam Technology and Materials Modification of Ministry of Education, College of Nuclear Science and Technology, Beijing Normal University, Beijing 100875, China
[b] Beijing Radiation Center, Beijing 100875, China
[c] Institute of Mechanics, Chinese Academy of Sciences, Beijing 100190, China

HIGHLIGHTS

- Electron temperature in plasma electrolytic carburizing process is determined.
- Diffusion coefficient of carbon in PEC is higher than conventional carburizing.
- Wear and corrosion resistance of T8 steel are both improved after PEC treatment.
- Pitting corrosion of steel substrate is obviously suppressed by PEC treatment.

ARTICLE INFO

ABSTRACT

A hardening layer of 70 μm on T8 carbon steel was fabricated by plasma electrolytic carburizing (PEC) in glycerol solution at 380 V with 3 min treatment. The discharge process was characterized using optical emission spectroscopy (OES), and the electron temperature in plasma envelope was determined. Meanwhile, diffusion coefficient of carbon was calculated on the basis of carbon concentration profile. The tribological property of carburized steel under dry sliding against ZrO_2 ball was measured by a ball-disc friction and wear tester. The corrosion behaviors were evaluated by potentiodynamic polarization and electrochemical impedance spectroscopy (EIS). It was found that the carburized layer mainly contained α-Fe and Fe_3C phases with maximum hardness of 620 HV. The PEC treatment significantly decreased the friction coefficient from 0.4 to 0.1. The wear rate of PEC treated steel was about 5.86×10^{-6} $mm^3/N \cdot m$, which was less than 1/4 of T8 steel substrate. After PEC treatment, the wear and corrosion resistance of T8 steel were improved. Particularly, the pitting corrosion of steel substrate was obviously suppressed.

© 2015 Elsevier B.V. All rights reserved.

1. Introduction

Chemical heat treatment methods such as carburizing, nitriding and carbonitriding have been developed to improve the surface hardness of steel materials. T8 high carbon steel, as a kind of carbon tool steel is widely used in the mould making due to its better processability and lower price. But conventional heat treatment including the pack carburizing and gas carburizing always leads to a large distortion of work pieces. Moreover, these methods usually carry out at high temperature up to 1000 °C or proceed in the vacuum environment, which results in high energy consumption and high cost [1–5]. In recent years, plasma electrolytic saturation (PES) technology has been studied as an efficient and environmentally friendly approach for surface hardening on metals [6]. Specific processing methods include plasma electrolytic carburizing (PEC), plasma electrolytic carbonitriding (PEC/N), plasma electrolytic borocarburizing (PEB/C) [7–9] and so on.

In the PES process, the work piece as cathode is immersed in organic electrolyte solution at ambient temperature. When the negative bias voltage is applied, the electrolyte solution is heated to

* Corresponding author. Key Laboratory for Beam Technology and Materials Modification of Ministry of Education, College of Nuclear Science and Technology, Beijing Normal University, Beijing 100875, China.
E-mail address: xuewb@bnu.edu.cn (W. Xue).

produce a continuous vapor envelope around the steel sample. By increasing the applied voltage to a critical value, the vapor envelope is broken down, resulting in plasma discharge at near-cathode region and an enhanced interstitial diffusion of active species like carbon, nitrogen and boron. Li et al. [10] successfully prepared a Ti(C$_x$N$_{1-x}$) film on titanium by PEC/N method in a mixed organic solution of triethanolamine and formamide. The film showed a good adhesion and high hardness. Tarakci et al. [11] produced a carburized layer on pure iron by PEC method. The hardness of the carbon-rich layer was significantly improved compared with the pure iron substrate. On this basis, Çavuşlu et al. [12] measured the wear rates of untreated and PEC treated pure iron. It showed that the carburized pure iron samples had lower wear rate and better wear resistance. However, the corrosion behavior of the PEC layer has not been evaluated. On the other hand, P. Belkin et al. [13] reported an anodic PEC treatment on carbon steel. There was a thick oxide layer covered on the carburized layer, but the carbon concentration was only 0.8 wt.% and the evaluation of layer performance was insufficient. So it is meaningful to examine the PEC layer properties combining wear and corrosion resistance.

In this paper, a carburized layer on T8 high carbon steel was rapidly fabricated by PEC method in an aqueous glycerol solution. Optical emission spectroscopy was employed to characterize the discharge phenomenon during PEC process. The microstructure, phase constituents and hardness profile of PEC treated steel were analyzed. The tribological behavior under dry sliding at ambient temperature and electrochemical performance were investigated. Besides, the carburization mechanism in PEC process was discussed.

2. Material and methods

A T8 high carbon steel (C: 0.75–0.84, Si: ≤0.35, Mn: ≤0.40, P: ≤0.035, S: ≤0.030, wt.%, Fe balance) plate with dimensions of 55 mm × 16 mm × 1 mm was used as substrate material. The plate was mechanically polished with 1000-grit emery paper, and then was cleaned in ethanol and dried. For the PEC treatment, a DC power supply was employed, and the T8 steel plate was used as cathode while a stainless steel container served as anode. The aqueous solution containing 80 vol.% glycerol was chosen as electrolyte. The negative bias voltage was initially set at 150 V to produce a continuous vapor envelope around the T8 sample. Then the applied voltage gradually increased and the vapor envelope was broken down at the critical voltage. When the voltage reached 380 V, the plasma discharge became stable. After 3 min treatment, the power supply was turned off slowly [14], and the T8 steel sample was cleaned in running water and dried.

During stable discharge, the active species in the plasma envelope were detected using optical emission spectroscopy (OES, AvaSpec-3648). The surface morphology and cross-sectional microstructure of PEC treated steel were observed by scanning electron microscope equipped with energy dispersive spectroscopy (SEM & EDS, Hitachi S-4800). A Vicker's microhardness tester with 10 g load was used to determine the hardness profile of PEC sample. The phase constituents of the sample before and after carburization were characterized by X-ray diffraction (XRD, X′Pert Pro MPD). A ball-disc friction and wear tester was employed to measure the tribological properties. The wear test was carried out under dry sliding with 5 N load against ZrO$_2$ ball of 4.763 mm in diameter. The surface roughness of samples and the cross-sectional profiles of wear tracks were measured by a surface profilometer equipped with a diamond stylus (TR200, Beijing Time Lianchuang technology Co., Ltd). Corrosion behaviors of PEC sample before and after polishing were evaluated using electrochemical workstation (PARSTAT 2273) in 3.5 wt.% NaCl aqueous solution. Potentiodynamic

polarization tests were performed at a scan rate of 1 mV/s. Electrochemical impedance spectroscopy (EIS) was carried out at the open circuit potential with an AC amplitude of 10 mV over the frequency range of 1 MHz to 0.01 Hz. A polishing machine with metallographic polishing cloth was employed to remove the residual carbon particles on the PEC specimen surface. The rotational speed of the polishing machine is 600 r/min. The surface roughness of the polished PEC specimen is 0.39 μm.

3. Results and discussion

3.1. Spectroscopic investigation of plasma discharge

According to the theory of atomic emission spectrum, during the transition of excited atoms from higher level to lower level, the energy will be released in the form of light radiation to generate OES spectrum. Fig. 1 shows a typical OES spectrum of the plasma discharge on T8 steel in glycerol aqueous solution. The plasma zone contains iron from steel substrate, and carbon, hydrogen, oxygen from electrolyte. Meanwhile, there are no strong signals below 350 nm wavelength, probably due to the self-absorption of light [15]. The H I refers to a neutral hydrogen atom, while the C II, Fe II and O II are singly ionized atoms. The emission intensity of active species can be utilized to indicate whether the plasma has produced the operation conditions required for a certain coating process. As far as this experiment is concerned, active Fe, H, O, C radicals and ionic components take part in the discharge reaction to fabricate a carburized layer on T8 steel, and carbon species are dominant during this process.

On the other hand, the plasma produced during PEC process belongs to a local thermal equilibrium (LTE) plasma. In the LTE state, the electron temperature (T_e) can be obtained from Eq. (1) when relative line intensities of the same atomic or ionic species are given [16].

$$\frac{I_1}{I_2} = \frac{A_1 g_1 \lambda_2}{A_2 g_2 \lambda_1} \exp\left(-\frac{E_1 - E_2}{kT_e} \right) \tag{1}$$

where I_1, A_1, g_1, λ_1, E_1 and I_2, A_2, g_2, λ_2, E_2 are relative intensity, transition probability, statistical weight of upper level, wavelength and excitation energy of the two emission spectral line, respectively, and k is the Boltzmann constant. Combined with the spectrum in Fig. 1, the Fe II lines at 516.65 nm and 697.57 nm are selected to determine the T_e. Corresponding parameters are listed in Table 1
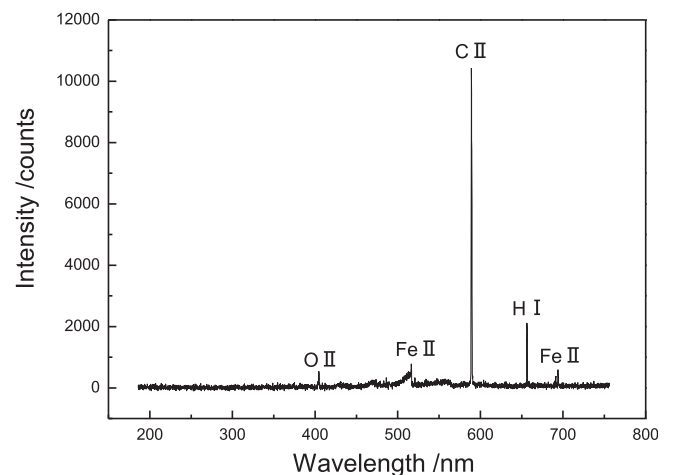

Fig. 1. Typical emission spectrum of PEC process on T8 steel in glycerol aqueous solution.

Table 1
Fe II lines with the wavelength, transition, statistical weights of upper level, energy difference between the two levels and transition probabilities.

Line	λ (nm)	Transition	g_k	Energy (eV)	A_{ki} (10^7 S^{-1})
Fe II	516.65	$3d^6(^5D_2)4f \rightarrow 3d^6(^5D)4d$	8	2.4	2.82
Fe II	697.57	$3d^6(5D)5d \rightarrow 3d^6(^5D)5p$	4	1.8	1.92

[17]. The calculated T_e is about 5000 K, which refers to a transient temperature of plasma discharge zone.

3.2. Morphology and microstructure of carburized layer

Fig. 2a is the surface micrograph of PEC treated steel with 3 min discharge. Some remained cavities and channels on the surface can be observed, which result from intense plasma etching during discharge process. Furthermore, the surface roughness of PEC treated steel becomes 0.56 μm while the steel substrate is only 0.18 μm. The EDS map of the surface is displayed in Fig. 2b. The C, O, Fe elements are detected on the surface of PEC treated steel. Fig. 3a shows the cross-sectional microstructure of the PEC treated steel. It consists of two layers: a carburized layer of about 30 μm and a carbon diffusion layer of about 40 μm. Active carbon atoms, decomposed from glycerol, permeate into the steel from surface to interior. Since the steel substrate far from the surface keeps relatively low temperature, the carbon diffusion is gradually suppressed and the carbon atoms accumulate in some regions. Then the residual carbon atoms diffuse along the grain boundary to form the diffusion layer due to the irregular atomic arrangement and
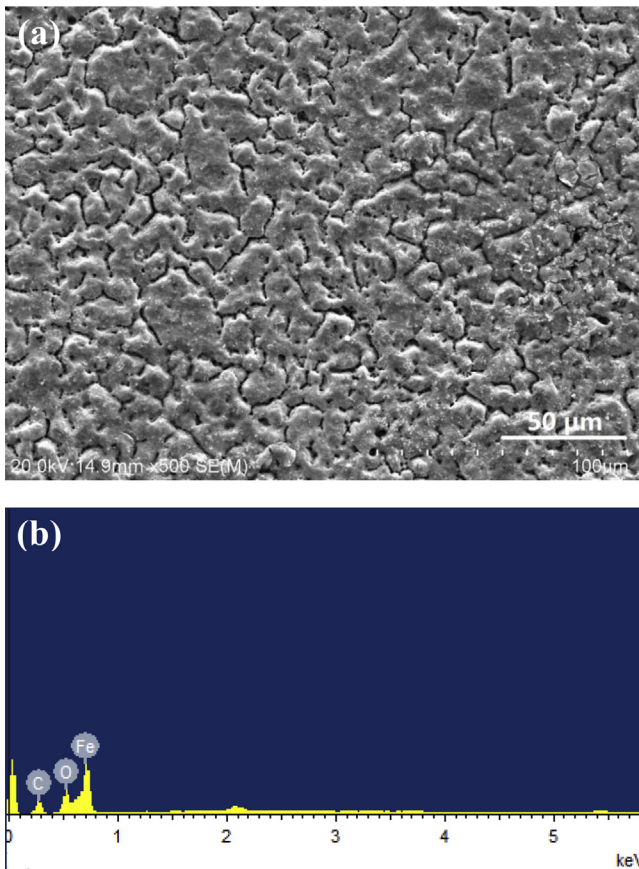
Fig. 2. (a) Surface morphology of the PEC treated steel with 3 min treatment. (b) Typical EDS map of the steel surface after PEC treatment.
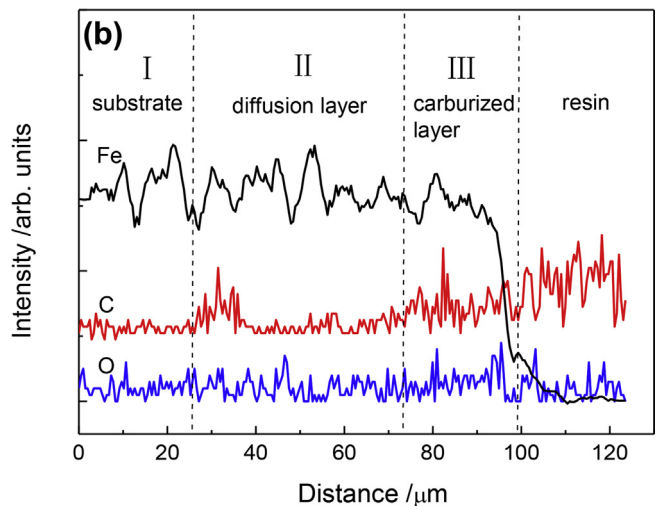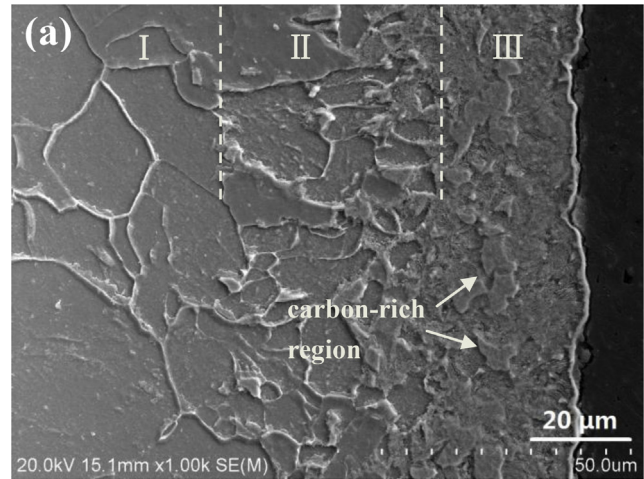
Fig. 3. (a) Cross-sectional microstructure of the PEC treated steel: I substrate, II diffusion layer, III carburized layer. (b) Composition distribution of Fe, C and O elements in the PEC treated steel.

loose structure in the grain boundary. Fig. 3b displays the composition profiles of Fe, C and O elements in the PEC treated steel. The carburized layer and diffusion layer can be distinguished by two carbon peaks. Their thicknesses are consistent with the cross-section image in Fig. 3a. The carbon peaks correspond to the carbon-rich regions, which are formed by carbon atoms accumulation during diffusion process. In addition, iron content decreases in carburized layer while oxygen content slightly increases.

As to Fig. 3a, a one-dimensional diffusion model for the Fick's second law is built and its error function solution is presented as Eq. (2).

$$C = C_S + (C_0 - C_S)erf\left(\frac{x}{2\sqrt{Dt}}\right) \tag{2}$$

The notation C refers to the carbon content in position x, while C_s and C_0 are the carbon content on the surface and in the interior of steel matrix, respectively. D is the diffusion coefficient of carbon atoms. In this simplified model, the steel sample is seen as semi-infinite, and the C_s remains unchanged approximately. Fig. 4 shows the distribution of carbon concentration in PEC layer by EDS composition analysis. It is found that the carbon concentration decreases from surface of PEC layer to steel substrate. The peak values originate from the carbon-rich regions in Fig. 3b. In terms of
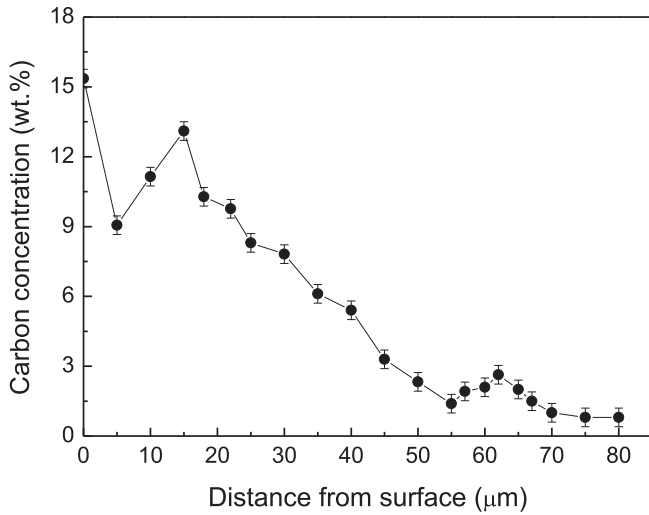
Fig. 4. Carbon concentration profile along the cross section of PEC treated steel.

Fig. 6. Microhardness distribution of PEC treated steel across the layer thickness.

Eq. (2), the relationship between diffusion distance (x) and carburizing time (t) can be derived, as shown in Eq. (3).

$$x = \sqrt{Dt} \qquad (3)$$

In this work, the x and t are 70 μm and 180 s, respectively. Thus the carbon diffusion coefficient can be calculated, and it turns out to be 2.72×10^{-7} cm^2 s^{-1}. As for the conventional carburizing process, the diffusion coefficient of carbon is determined by carburizing temperature. Eq. (4) depicts the relationship between diffusion coefficient (D) and carburizing temperature (T). The D_0 and Q are constants, given by Ref. [1].

$$D = D_0 \exp\left(-\frac{Q}{RT} \right) \qquad (4)$$

The carburizing temperature during PEC process is 793.6 °C, which is measured by inserting a thermocouple into the sample. At this temperature, the diffusion coefficient in conventional carburizing process is 1.81×10^{-8} cm^2 s^{-1}, which is one magnitude lower than the diffusion coefficient of PEC process.
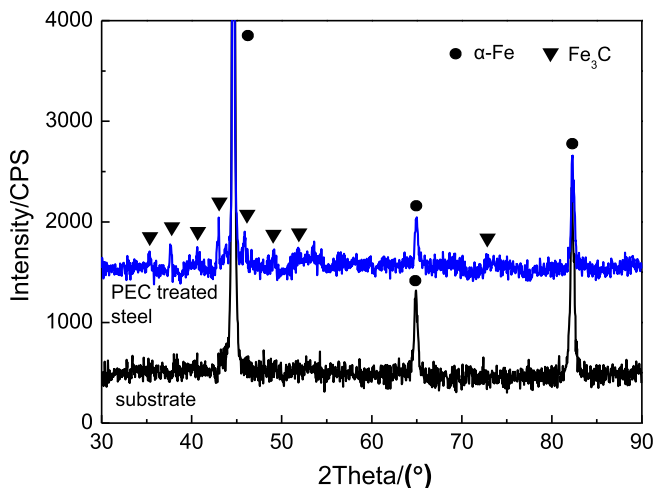
3.3. Phase constituents analyses and hardness profile of PEC treated steel

Fig. 5 displays the XRD patterns of T8 steel before and after PEC treatment. There is only ferrite (α-Fe) phase in T8 substrate, but in

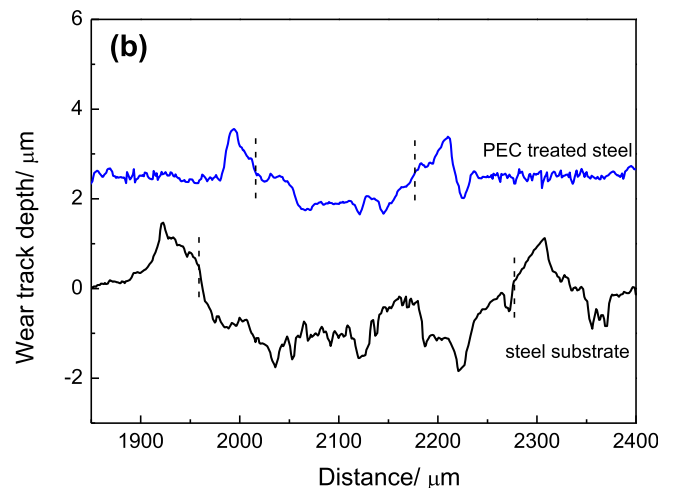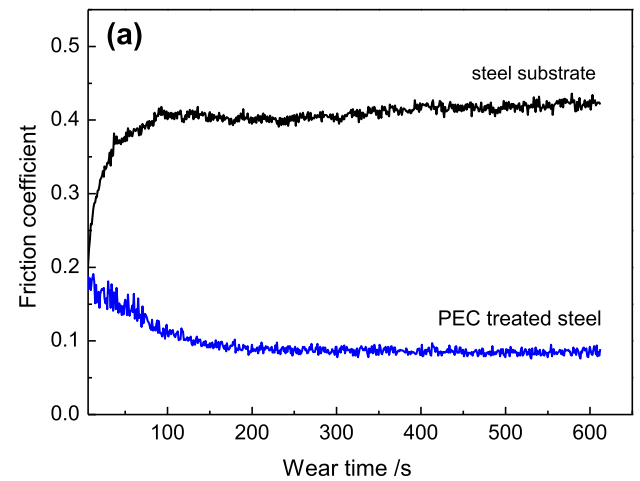**Fig. 5.** XRD patterns of bare T8 steel substrate and the PEC treated steel.

Fig. 7. Friction coefficient (a) and cross-sectional profiles of wear tracks (b) for T8 steel substrate and PEC treated steel against ZrO$_2$ ball with 5 N load.

the PEC treated steel some Fe_3C peaks are detected. The phase constituents of PEC treated steel is similar to that of the conventional gas carburizing technique [18]. It means that the carbon species, decomposed from glycerol through plasma discharge, has diffused into the steel and formed the cementite by precipitating.

The cross-sectional hardness profile of PEC treated steel at 10 g load is shown in Fig. 6. It is found that the microhardness gradually increases from the steel substrate to the surface of hardening layer. The maximum hardness appears in the carburized layer and corresponds to the carbon accumulated regions or carbon-rich regions in Fig. 3a. The maximum hardness of carburized layer is about 620 HV, which is more than five times of the steel substrate (110 HV). It is believed that the high hardness should be ascribed to the appearance of Fe_3C hard phase as revealed in Fig. 5.

3.4. Tribological performance of PEC treated steel

Fig. 7a depicts the friction coefficient of T8 steel substrate and PEC treated steel under dry sliding against ZrO_2 ball with 5 N load at ambient temperature. At the stable wear stage, the friction coefficient of PEC sample is about 0.1, which is much lower than that of bare steel with about 0.4. Fig. 7b reveals the cross-sectional profiles of wear tracks measured by a surface profilometer. It is clear that the area of wear track for steel substrate is larger than that of PEC treated steel. According to the calculation result, the wear rate of PEC treated steel is about 5.86×10^{-6} mm^3/N m, which is less than 1/4 of T8 steel substrate. The low friction coefficient and good wear resistance of PEC treated steel are ascribed to the high hardness of carburized layer and the lubrication action of remained carbon particles distributed on the surface.

The surface morphologies of wear tracks on T8 steel substrate and PEC treated steel are shown in Fig. 8a and c. Magnified images are respectively displayed in Fig. 8b and d. Compared with the steel substrate, the wear track of PEC treated steel is narrower, which is consistent with the cross-sectional profiles in Fig. 7b. Furthermore, some parallel grooves and severe peeling can be observed on the substrate surface, suggesting that abrasive wear occurs during the wear test. Besides, the oxygen content of peeled area in Fig. 8b is high. Table 2 shows the compositions of the worn surface of steel substrate and PEC treated steel. The concentrations of O and Zr in the dark region A are higher than those in the bright region B. Because the friction heat causes local oxidation of the worn surface, and more Zr element is transferred into dark regions due to longer contact time with ZrO_2 ball. In addition, the O and Zr contents of PEC treated steel are lower than those of bare steel substrate. This indicates that the oxidation and material transfer for the PEC sample are weaker than those for the bare steel substrate. Meanwhile, the wear track of the PEC treated steel is smooth with some fatigue cracks. The fatigue cracks are pointed out by white arrows in Fig. 8d. The wear mechanism has transformed to oxidation wear and fatigue wear.

3.5. Corrosion behavior of PEC treated steel

Fig. 9a shows the polarization curves of T8 steel substrate and PEC treated steel. The corrosion potential (E_{corr}), corrosion current density (i_{corr}) and polarization resistance (R_p) are listed in Table 3. It reveals that both the E_{corr} and i_{corr} of PEC treated steel are lower than steel substrate. Thus, the corrosion resistance of PEC treated steel is improved since the polarization curve moves towards the region of lower current density. In addition, after gently polishing the surface of PEC sample, the i_{corr} decreases slightly from 6.84×10^{-6} to 5.72×10^{-6} A/cm^2, while the E_{corr} increases markedly from -0.5964 to -0.5065 V. Though the i_{corr} might be affected
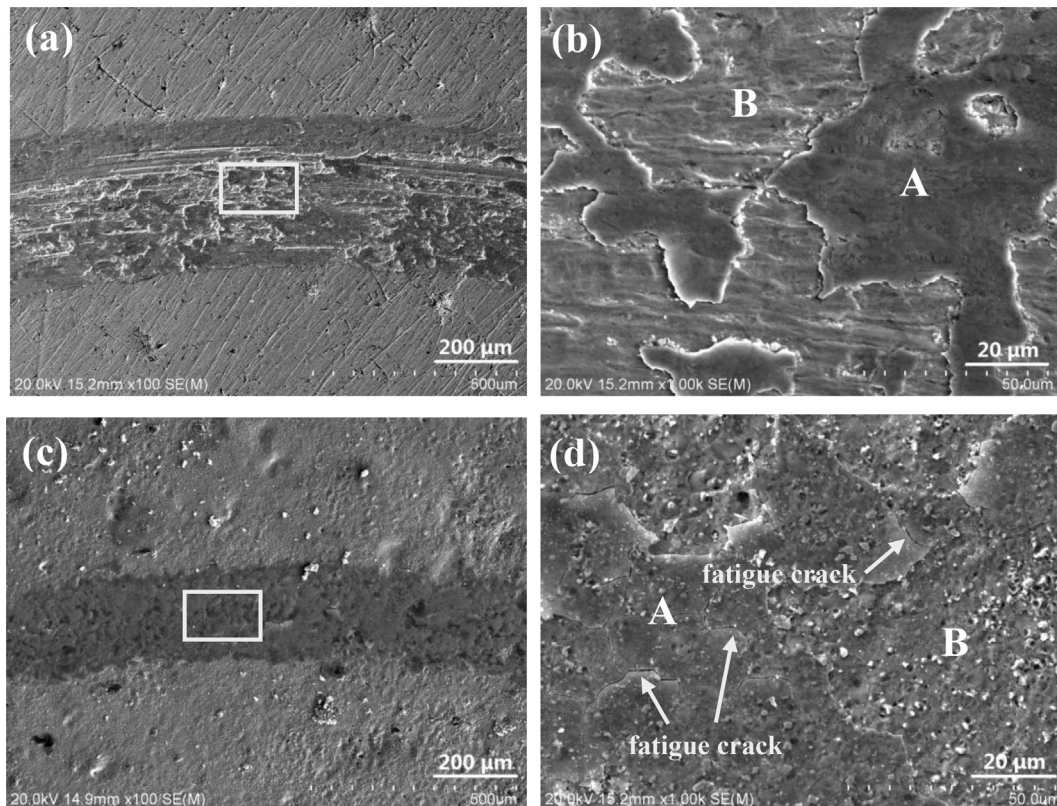

Fig. 8. Morphologies of the wear tracks on T8 steel substrate (a) and PEC treated steel (c); (b) and (d) are the magnification of (a) and (c), respectively.

Table 2
EDS analyses of the worn surface on steel substrate and PEC treated steel.

Weight percentage %	O		Fe		Zr	
	Region A	Region B	Region A	Region B	Region A	Region B
Steel substrate	24.37	11.13	72.84	88.87	2.79	0
PEC treated steel	10.99	4.37	88.86	95.62	0.15	0.01

by the reduced surface area of the specimen after polishing, the increase of E_{corr} implies that the corrosion resistance of the polished PEC steel is improved compared with the unpolished PEC steel. On the other hand, Fig. 9b shows the typical Nyquist plots of steel substrate and PEC treated steel. Their equivalent circuits are proposed in Fig. 9c and d, respectively [19] and the fitting results are listed in Table 4. R_s is solution resistance, C_{dl} is double layer capacitance, R_t is charge transfer resistance, CPE and R_f are constant phase element and resistance of passive film on steel formed in aqueous solution. CPE is defined as $Z_{CPE} = 1/[Y_0(j\omega)^n]$, where Y_0 is modulus of admittance, ω is perturbing frequency and n is an exponent to characterize the deviation degree of real capacitance
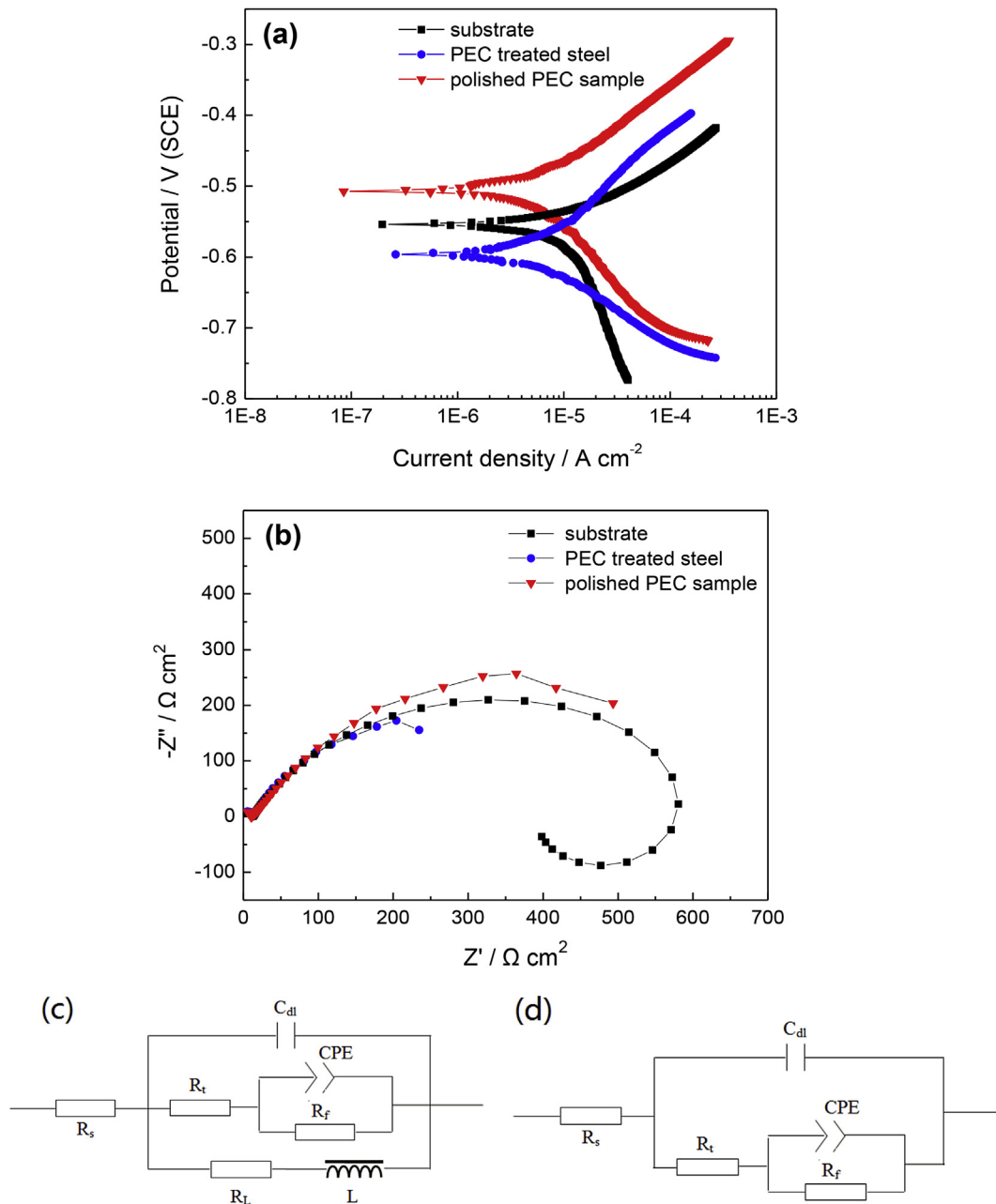

Fig. 9. Potentiodynamic polarization curves (a) and Nyquist plots (b) of T8 steel substrate and PEC treated steel in 3.5 wt.% NaCl aqueous solution. (c) Equivalent circuit diagram for EIS plot of T8 steel substrate. (d) Equivalent circuit diagram for EIS plot of PEC treated steel.

Table 3
Fitting results of potentiodynamic polarization curves of T8 steel substrate and PEC treated steel before and after polishing.

	E_{corr} (V)	i_{corr} (A/cm^2)	R_p (Ω/cm^2)
Substrate	−0.5554	1.19×10^{-5}	2543
PEC treated steel	−0.5964	6.84×10^{-6}	4108
Polished PEC sample	−0.5065	5.72×10^{-6}	5349

Table 4
Fitting results of EIS plots of T8 steel substrate and PEC treated steel before and after polishing.

	R_s Ω cm^2	C_{dl} F cm^{-2}	R_t Ω cm^2	CPE, Y_0 Ω^{-1} cm^{-2} s^{-n}	n	R_f Ω cm^2	R_L Ω cm^2	L H cm^2
Substrate	0.01	1.562×10^{-8}	12.67	5.474×10^{-4}	0.7192	589	874	4251
PEC treated steel	0.01	1.227×10^{-8}	12.78	1.783×10^{-2}	0.7476	530		
Polished PEC sample	0.01	1.194×10^{-8}	1.142	6.093×10^{-3}	0.6579	981		

from its ideal value ($0 < n \leq 1$) [20,21]. R_L and L are inductance resistance and inductance corresponding to the pitting formation.

The sensitivity of pitting corrosion can be estimated by the EIS plots before the pitting corrosion really occurs. As for the T8 steel substrate, the appearance of inductive loop at low frequency (see Fig. 9b) means that the pitting corrosion is easy to take place on bare steel. After the PEC treatment, the inductive loop in EIS plot does not appear, which implies that the carburized layer can suppress the occurrence of pitting. On the other hand, the capacitive loop diameter of the PEC treated steel is similar to that of T8 steel substrate. After gently polishing the sample surface, the polished PEC sample exhibits a better corrosion resistance compared with the bare steel substrate and the unpolished sample, since the carbon particles have been removed from the surface. The capacitive loop diameter of polished PEC sample is larger and the R_f with 981 Ω cm^2 is higher than that of T8 steel substrate. Therefore, the PEC treatment improves the corrosion resistance of steel, which is consistent with the polarization results. Particularly, PEC treatment can suppress the occurrence of pitting corrosion for T8 steel.

Based on the above discussion, the carburization mechanism in PEC process can be summarized as follows. When the applied voltage is initially set at 150 V, the T8 steel surface is heated and a continuous vapor envelope containing hydrogen and glycerol molecules is formed around the steel sample. As the voltage increases, the high voltage mainly concentrates on the thin gas envelope with low electrical conductivity. Then the breakdown of gas envelope occurs at a critical voltage, resulting in the plasma discharge at the near-cathode region. At 380 V, the plasma discharge becomes stable and more glycerol is decomposed, releasing C, H and O reactive species on the surface of steel substrate. These active radicals and ionic components are accelerated by the strong electric field, generating an enhanced interstitial diffusion into the iron lattice. Consequently, Fe$_3$C phase appears and a carburized layer is formed with the increase of discharge time. Furthermore, this hard and compact carburized layer not only improves the wear resistance of steel, but also effectively protects the steel substrate against pitting corrosion in NaCl aqueous solution.

4. Conclusions

Plasma electrolytic carburizing can form a carburized layer with

thickness about 30 μm on T8 high carbon steel by 3 min discharge treatment at 380 V in glycerol solution. Below the carburized layer, there is a 40 μm thick diffusion layer, which is caused by carbon diffusing along the grain boundary. Diffusion coefficient of carbon atoms into steel during PEC process is calculated to be 2.72×10^{-7} cm^2 s^{-1}, while electron temperature in plasma discharge zone is about 5000 K. The carburized layer mainly contains α-Fe and Fe$_3$C phases and the maximum hardness is about 620 HV. The PEC treatment greatly improves wear resistance of steel. The corrosion resistance is also improved and the pitting corrosion of steel substrate is obviously suppressed.

References

[1] H. Jiménez, M.H. Staia, E.S. Puchi, Surf. Coat. Technol. 120–121 (1999) 358–365.
[2] M.F. Yan, Mater. Chem. Phys. 70 (2001) 242–244.
[3] X.Y. Li, N. Habibi, T. Bell, H. Dong, Surf. Eng. 23 (2007) 45–51.
[4] B. Suh, W. Lee, Thin Solid Films 295 (1997) 185–192.
[5] T. Christiansen, M.A.J. Somers, Surf. Eng. 21 (2005) 445–455.
[6] A.L. Yerokhin, X. Nie, A. Leyland, A. Matthews, S.J. Dowey, Surf. Coat. Technol. 122 (1999) 73–93.
[7] J. Wu, W. Xue, B. Wang, X. Jin, J. Du, Y. Li, Surf. Coat. Technol. 245 (2014) 9–15.
[8] C. Tsotsos, A.L. Yerokhin, A.D. Wilson, A. Leyland, A. Matthews, Wear 253 (2002) 986–993.
[9] B. Wang, W. Xue, J. Wu, X. Jin, M. Hua, Z. Wu, J. Alloys Compd. 578 (2013) 162–169.
[10] X. Li, Y. Han, Electrochem. Commun. 8 (2006) 267–272.
[11] M. Tarakci, K. Korkmaz, Y. Gencer, M. Usta, Surf. Coat. Technol. 199 (2005) 205–212.
[12] F. Çavuşlu, M. Usta, Appl. Surf. Sci. 257 (2011) 4014–4020.
[13] P.N. Belkin, Surf. Eng. Appl. Electrochem. 46 (2010) 558–569.
[14] J. Wu, R. Liu, W. Xue, B. Wang, X. Jin, J. Du, Appl. Surf. Sci. 316 (2014) 102–107.
[15] R.O. Hussein, X. Nie, D.O. Northwood, A. Yerokhin, A. Matthews, J. Phys. D. Appl. Phys. 43 (2010) 105203.
[16] R. Liu, J. Wu, W. Xue, Y. Qu, C. Yang, B. Wang, X. Wu, Mater. Chem. Phys. 148 (2014) 284–292.
[17] http://physics.nist.gov/PhysRefData/ASD/lines_form.html.
[18] C.J. Scheuer, R.P. Cardoso, F.I. Zanetti, T. Amaral, S.F. Brunatto, Surf. Coat. Technol. 206 (2012) 5085–5090.
[19] C. Zhong, X. Tang, Y.F. Cheng, Electrochim. Acta 53 (2008) 4740–4747.
[20] F. Cao, J. Cao, Z. Zhang, J. Zhang, C. Cao, Mater. Corros. 58 (2007) 696–703.
[21] T. Chen, W. Xue, Y. Li, X. Liu, J. Du, Mater. Chem. Phys. 144 (2014) 462–469.